Experimental investigation into the sealing capability of naturally fractured shale caprocks to supercritical carbon dioxide flow

Experimental investigation of supercritical Carbon Dioxide flow behaviour through naturally fractured caprocks

K. Edlmann*, S. Haszeldine and C. I. McDermott

*Addresses for correspondence:

Katriona Edlmann
School of GeoSciences,
University of Edinburgh,
West Mains Road,
Edinburgh, UK
EH9 3JW

Experimental investigation into the sealing capability of naturally fractured shale caprocks to supercritical Carbon Dioxide flow

Authors

K. Edlmann [1], S. Haszeldine [1], C.I. McDermott [1,2]

[1]*Edinburgh Collaborative of Subsurface Science and Engineering (ECOSSE), School of Geoscience, University of Edinburgh, West Mains Road, Edinburgh, EH9 3JW, United Kingdom*

[2]*Centre for Science at Extreme Conditions, University of Edinburgh, Erskine Williamson Building, The King's Buildings, Mayfield Road, Edinburgh EH9 3JZ, United Kingdom*

Abstract

Geological storage of CO_2 is considered a solution for reducing the excess CO_2 released into the atmosphere. Low permeability caprocks physically trap injected CO_2 injected into underlying porous reservoirs. Injection leads to increasing pore pressure and reduced effective stress, increasing the likelihood of exceeding the capillary entry pressure of the cprocks and of caprock fracturing. Assessing how CO_2 flows through the caprock matrix and fractures in all its phases is important for assessing CO_2 storage security. Fractures are considered to represent preferential flow paths in the caprock for the escape of CO_2. Here we present a new experimental rig which allows 38mm diameter fractured caprock samples recovered from depths of ~4 km to be exposed to supercritical CO_2 ($scCO_2$) under in-situ conditions of pressure, temperature and geochemistry. Contrary to expectations, the results indicate that $scCO_2$ will not flow through tight natural caprock fractures, even with a differential pressure across the fractured sample in excess of 51 MPa. However below the critical point where CO_2 enters its gas phase, the CO_2 flows readily through the caprock fractures. This indicates the possibility of a critical threshold of fracture aperture size which controls CO_2 flow along the fracture.

Keywords

CO_2 geological storage

Caprock leakage

Supercritical CO_2 experiments

Fracture aperture

Capillary entry pressure

1. Introduction

Concentrations of atmospheric CO_2 have increased by more than 35% since industrialisation began (UK Met Office 2010). Current global demand for fossil fuels is 80% of the total energy requirement (International Energy Agency 2008).

To reduce the amount of CO_2 entering the Earth's atmosphere from increasing energy demands, Carbon Capture and Storage in deep geological formations is being considered. CO_2 is separated from industrial emissions and injected in its supercritical phase (or dense phase) into suitable deep geological formations. CO_2 saturated fluids and separated phase CO_2 are held in porous rocks sealed by overlying impermeable caprocks (Koide at al, 1992). Understanding the long term integrity of these caprock seals is a pre-requisite for CO_2 storage, Bachu (2003), Li et al. (2005 & 2006), Class (2009), Ketzer et al. (2009), Fischer et al. (2010), Gaus (2010) and Amann et al. (2011).

There are four mechanisms that trap CO_2 (e.g. Chadwick et al., 2008). Dissolution trapping occurs when injected CO_2 dissolves within the reservoir brine. Over long time periods this dissolved CO_2 can react with rock minerals or pore fluids to form other minerals or aqueous complexes resulting in geochemical trapping. Residual saturation trapping occurs when ganglia of CO_2 are trapped within pore spaces due to capillary forces, or adsorbed onto mineral grains. However the predominant trapping mechanism is considered to be structural trapping (Gunter et al., 2004), where the caprock acts as a mechanical barrier both in terms of its low permeability and its high capillary entry pressure, (Schowalter 1981, Schlomer and Kroos 1997 and Wollenweber et al. 2009).

It is generally accepted that leakage through the caprock during CO_2 injection and storage could occur through three processes:

a) Diffusion of CO_2 through the water saturated caprock. However work by Angeli et al (2009), Wollenweber at al. (2010) and Busch et al. (2010) have shown that diffusive losses through the caprock matrix are negligible during CO_2 storage conditions.

b) Exceeding the capillary entry pressure with the leakage of CO_2 through the interconnected flow paths through the pore system of the cap rock. Busch (2010) has shown that under an overpressure of 2 MPa above the capillary entry pressure CO_2, breakthrough of the caprock occurs after hundreds to thousands of years for medium to low permeability caprocks with a realistic thickness of 100m. This is in line with findings by Deming (1994). The above findings suggest that as long as injected fluid pressures do not exceed the capillary entry pressures there should be minimal capillary flow leakage through the caprock pore network under CO_2 storage conditions.

c) Fracture flow. Natural fractures can offer preferential flow paths through the caprock. In additionthe increase in formation pressure could result in the reactivation of pre-existing faults / fractures, induce hydro fracturing and instigate shear fracturing in the overlying caprock. These fractures could become CO_2 leakage conduits.

Of these three mechanisms the issue of flow though natural and induced fractures presents a large risk to storage integrity and requires further investigation. Laboratory experiments have shown that increasing pore fluid pressure in caprocks reduces their strength and can induce brittle failure (Handin et al. 1963, Blanpied et al. 1992 and Nygard et al. 2006). Increasing pore fluid pressure (P_f) leads to lower effective stress $\sigma' = (\sigma - P_f)$. Effective normal stresses ($\sigma n - P_f$) press fault blocks together and thereby develop frictional resistance to any movement (shear) along the fault. Higher pore pressures decrease the normal stress across the fault lowering the frictional resistance to sliding and can lead to shearing. Hydro fracturing is thought to occur when the pore fluid pressure below the top seal equals or exceeds the minimum horizontal stress plus the tensile strength of the caprock, e.g. Watts (1987).

The injection of CO_2 also induces temperature alterations leading to thermal stresses which, depending on the rock mass characteristics at a local scale, can be similar or greater than the tectonic stresses, (McDermott et al. 2006) and lead to thermal fracturing.

Fracture surfaces are multi-faceted and can become either barriers or conduits to flow. To assess the transmissibility of a fracture three methods can provide an indication of the sealing capability of the fracture surface:

- Clay smear potential (Bouvier et al, 1989).
- Shale smear factor (Lindsay et al, 1993).
- Shale gouge ratio (Yielding et al, 1997).

All three methods are based on estimates of the distribution of clay along faults and highlight that a clay rich fracture surface will add its own complexity to the multiphase flow of formation fluids and injected CO_2 across a fracture surface.

In this paper we present the results of experimental investigation into the sealing properties of naturally fractured caprocks under in-situ conditions to supercritical CO_2 and gas phase CO_2 flow. A number of caprock samples have been collected from the North Sea East Brae field at a depth of circa 4km, and placed under of pressure and temperature representative of a typical CO_2 storage site. Naturally fractured samples are extremely rare as they are both very expensive to obtain, and natural fractures are rarely drilled through and preserved. Here the results of the investigation into two different fractured samples are presented along with those of another unfractured sample.

2. Experimental method

2.1. Sample selection & characteristics

The Kimmeridge clay caprock used in this study is from the North Sea East Brae Field. This lies at the western margin of the South Viking Graben. The East Brae field is an Upper Jurassic gas condensate reservoir, interpreted as a basin floor turbidite sediment enclosed by Kimmeridge Clay, Branter (2003). The Kimmeridge Clay is a clay rich siltstone with micaceous laminae, the porosity ranges between 20% to 5%, decreasing with depth, permeabilities are in the region of 4nD to 0.09nD and pore sizes from 11nm to 6nm (Okiongbo, 2011 and Yang & Aplin, 2007). Wellbore core samples of Kimmeridge clay caprock were obtained from Well 16/3a-E1 from depths of 3910m to 3918m.

2.2. Sample preparation

Borehole core from 4km depth identified as containing natural fractures was re-cored and the ends trimmed to provide two intact 38mm diameter cylindrical samples. Both samples contain natural fractures that run end to end lenthways through the sampe, (Sample B-a and B-b). A non-fractured sample, B-c was also obtained from the core, Figure 1. Table 1 presents the available dimensions, porosity, pore radius and permeability data for the three caprock samples and the average properties for the Kimmeridge Clay. After the CO2 flow experiment a 2 mm slice was removed from the upstream side sample B-a for SEM analysis to identify any mineralogy effects in the fractured caprock to CO2 exposure.

	Sample diameter (mm)	*Sample length (mm)*	*Water saturated weight (g)*	*Corrected porosity (%)*	*mean pore radius (nm)*	*90% percentile pore radius (nm)*
Sample B-a	38	49.6	132.3	16	811	34.3
Sample B-b	37.9	54.1	144.5	17	1075	118
Sample B-c	38.1	60.5	173.1	16	976	97.6

Table 1: Hg-porosimetry results for Samples B-a, B-b and B-c.

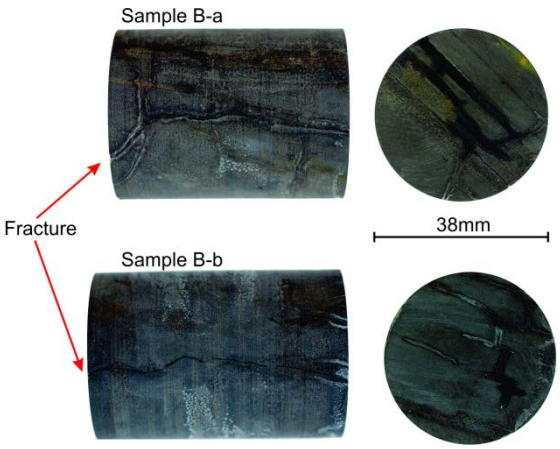

Figure 1: Images of the two 38mm diameter core samples of naturally fractured caprock from East Brae.

2.3. Mineralogical composition

X-Ray Diffraction investigations of both the caprock matrix and fracture fill material show that quartz (43%) and illite (≈25%) are the primary minerals that make up the Kimmeridge clay caprock, with minor chlorite (8%) and kaolinite (8%), Table 2. SEM images of the Kimmeridge Clay caprock microstructure show that quartz grains of up to 10μm are disseminated in the clay matrix. There is a definite bedding orientation of the matrix material (Figure 2A) with discrete quartz and pyrite crystals (Figure 2B).

	Qz	*Calcite*	*Dolomite*	*Albite*	*Illite*	*Kaolinite*	*Chlorite*	*Microcline*	*Orthoclase*	*Muscovite*	*Pyrite*
Matrix	43.7	0.0	1.5	2.8	28.7	7.6	7.6	2.5	1.4	2.2	2.0
Fracture	43.8	0.8	4.2	3.1	22.9	8.5	8.2	2.7	1.5	2.1	2.2

Table 2: The % mineral abundances for caprock Sample B-a

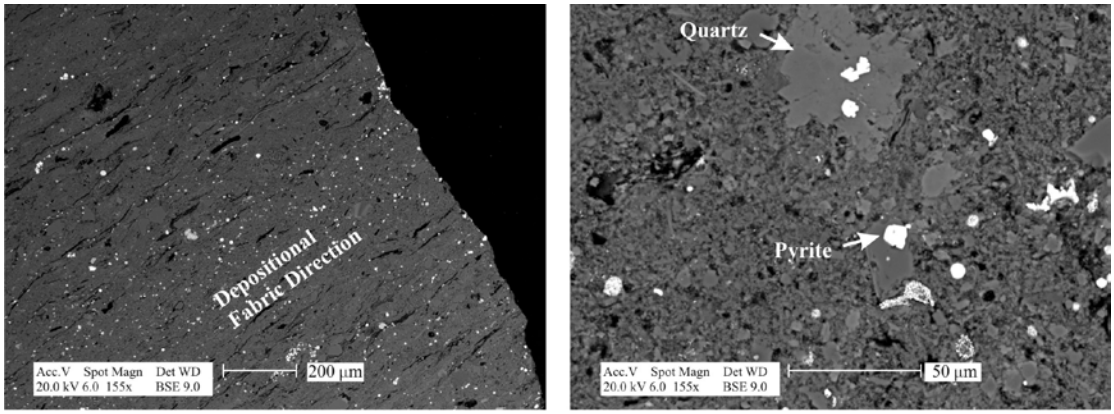

(A) Depositional Fabric

(B) Quartz and pyrite crystals

Figure 2: SEM backscatter images of the East Brae Kimmeridge Clay caprock showing depositional fabric (A) and quartz and pyrite crystals (B)

The mineral composition varies slightly for the fracture with the appearance of calcite and a higher percentage of dolomite along with a decrease in illite and to a lesser extent kaolinite and chlorite. In addition the % of illite is greater than muscovite and the % of kaolinite is higher than that of orthoclase. These factors can be explained as being a result of alteration of the fracture surface, indicating historical fluid flow along the fracture.

3. Experimental procedure

3.1. Sample saturation

The naturally fractured caprock samples were vacuum saturated in deionised water for 4 weeks and weighed to ensure the maximum saturation possible was reached. The samples were then placed into the experimental apparatus described below under in-situ conditions of pressure and temperature.

3.2. Experimental apparatus

The experimental rig was designed and built to facilitate multi-phase flow through 38mm diameter cylindrical rock samples over a range of temperatures, fluid types, fluid pressures and confining stress. It also allows the injection of tracers and other such markers along with fluid and gas sample collection post rock contact, (Figures 3 and 4).

The equipment consists of a Hassler-type high pressure vessel which holds cylindrical rock samples of 38mm diameter and up to 100mm in length. The fluid pumps (both brine and CO_2) are designed for high temperature, pressure and supercritical CO_2 conditions and all wetting parts within the system are in 316 stainless steel or PEEK to limit corrosion on exposure to brine and supercritical CO_2. The experimental equipment is rated to provide:

- Up to 69MPa radial confining ($\sigma 2=\sigma 3$) pressure.
- Up to 69MPa fluid pressure.
- Up to 80^{o}C fluid and rock temperature.
- Supercritical, liquid and gas phase CO_2 and brine fluid flow (both single and multi-phase).

- Upstream, downstream and differential pressure measurement and logging.

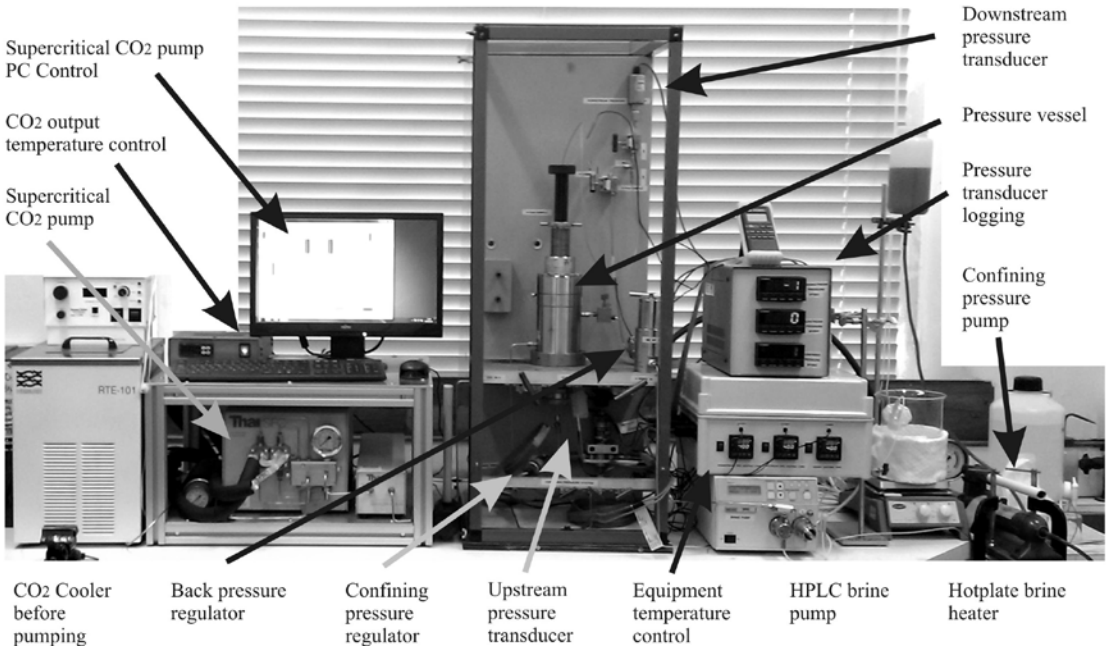

Figure 3: Image of the supercritical CO_2 flow rig designed and built at the University of Edinburgh

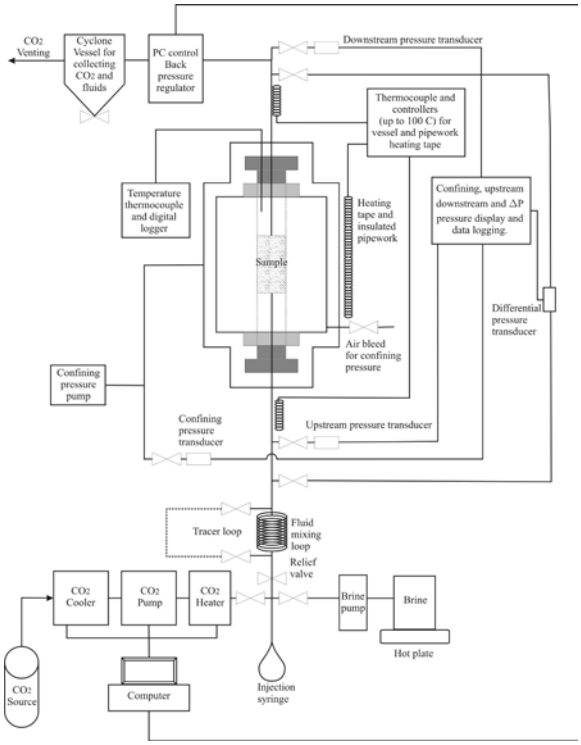

Figure 4: Schematic diagram of the experimental rig designed and built at the University of Edinburgh.

3.3. Experimental Programme

3.3.1. CO_2 flow program

The samples were loaded into the pressure vessel, the $scCO_2$ pump set to a constant flow rate of 1g/min and the pipework, vessel and rock temperature maintained at 40^oC via heating tapes and thermocouples. An automatic back pressure regulator downstream of the sample was set to 10 MPa. The following experimental program phases were followed:

Phase 1 – Reaching in-situ $scCO_2$ conditions: Once the system reached supercritical conditions the upstream CO_2 pressure was increased in 10 MPa increments from 20 MPa to 50 MPa. The radial confining pressure was also increased incrementally in line with the increasing fluid pressure. This ensured the confining pressure was always at least 5 MPa greater than the fluid pressure so that no leakage between the sample and the confining rubber sleeve of the pressure vessel was possible.

Phase 2 – Maintaining in-situ $scCO_2$ conditions: In this phase the fluid pump was switched off and the samples were locked into the pressure vessel and held constantly above the supercritical point for 30 days at 10 MPa upstream fluid pressure, 40^oC and 25 MPa confining pressure.

Phase 3 – Return to gas phase CO_2 conditions: After 30 days the upstream fluid pressure, confining pressure and fluid temperature were dropped below the critical point in a controlled manner to minimise any critical point phase change effects into the gas phase region and held constant at 6 MPa upstream fluid pressure, 20^oC and 15 MPa confining pressure for a further 30 days. Downstream pressure was set to 5 MPa to facilitate gas phase CO_2 flow.

Phase 4 – Return to $scCO_2$ in-situ conditions: Re-run of the increasing upstream CO_2 fluid pressure and lock in under supercritical conditions to identify if any wettability changes on the fracture surface occurred during exposure to gas phase CO_2 which would influence flow characteristic of $scCO_2$

3.3.2. Control Samples

To ensure there was no leakage of CO_2 along the side of the sample, between the sample and the confining rubber sleeve of the pressure vessel a solid non porous 38 mm diameter stainless steel cylinder control sample was subjected to the CO_2 flow program. There was no measurable flow across the steel sample under supercritical and gas phase CO_2.

To identify if any flow measurements were related to caprock matrix flow a water saturated non-fractured caprock sample, Sample B-c was subjected to the same CO_2 flow program as the fractured samples. Sample B-c, (Figure 5) has a diameter of 38.1 mm, a length of 60.5 mm and a water saturated weight of 173.1 g.

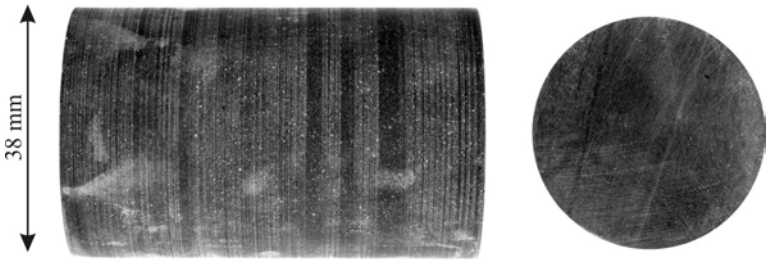

Figure 5: Image of the 38mm diameter core non fractured caprock sample, B-c from the North Sea Brae field.

There was no quantifiable flow measurements across the non-fractured caprock sample under $scCO_2$ and gas phase CO_2, Figure 6. This ensured that all pressure and flow measurements were directly related to the caprock fracture.

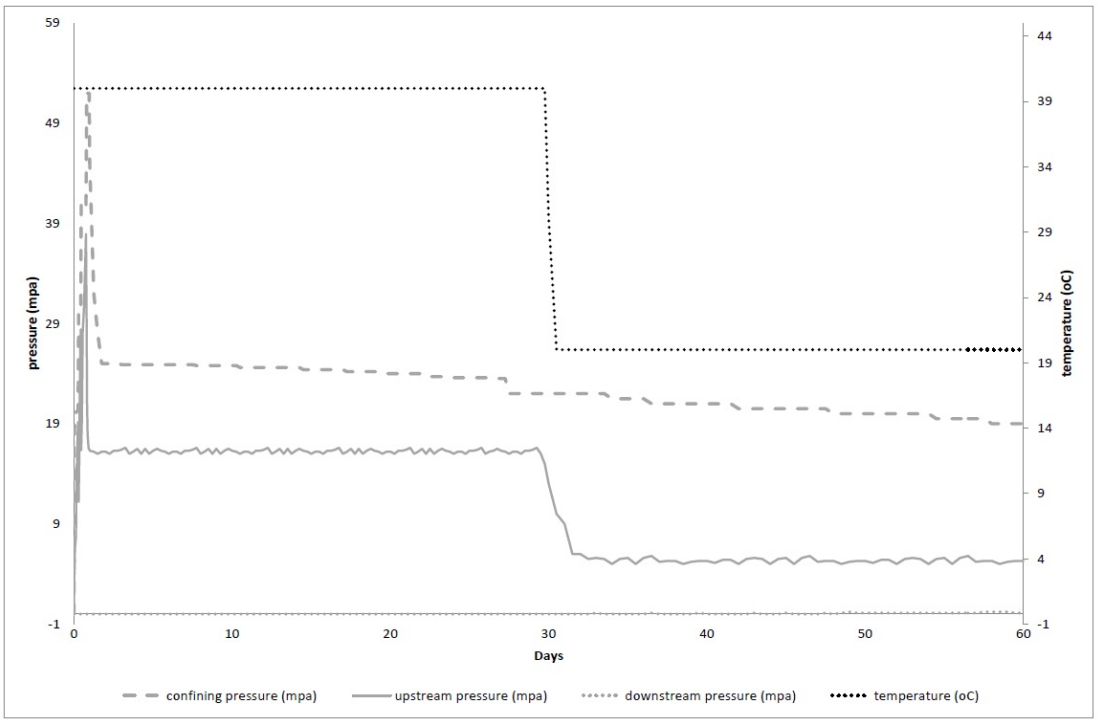

Figure 6: Pressure plot for supercritical CO_2 flow experiment on a non-fractured Kimmeridge Clay sample.

4. Results

Results are presented as temperature (^{o}C), confining pressure (MPa), upstream pressure (MPa), downstream pressure (MPa) and differential pressure (MPa) with time for the experiment phases.

4.1. Phase 1: Supercritical CO_2 flow experiment results

The upstream CO_2 fluid pressure was increased in 10 MPa increments from 20 MPa to 50 MPa and the upstream and downstream pressures were measured and logged.

There was no detectable flow (pressure) of scCO_2 measured across both fractured samples, even with a pressure differential of 43 MPa and 51 MPa and a pressure gradient of 866 MPa/m and 942 MPa/m for samples B-a and B-b respectively, Figures 7a and 7b.

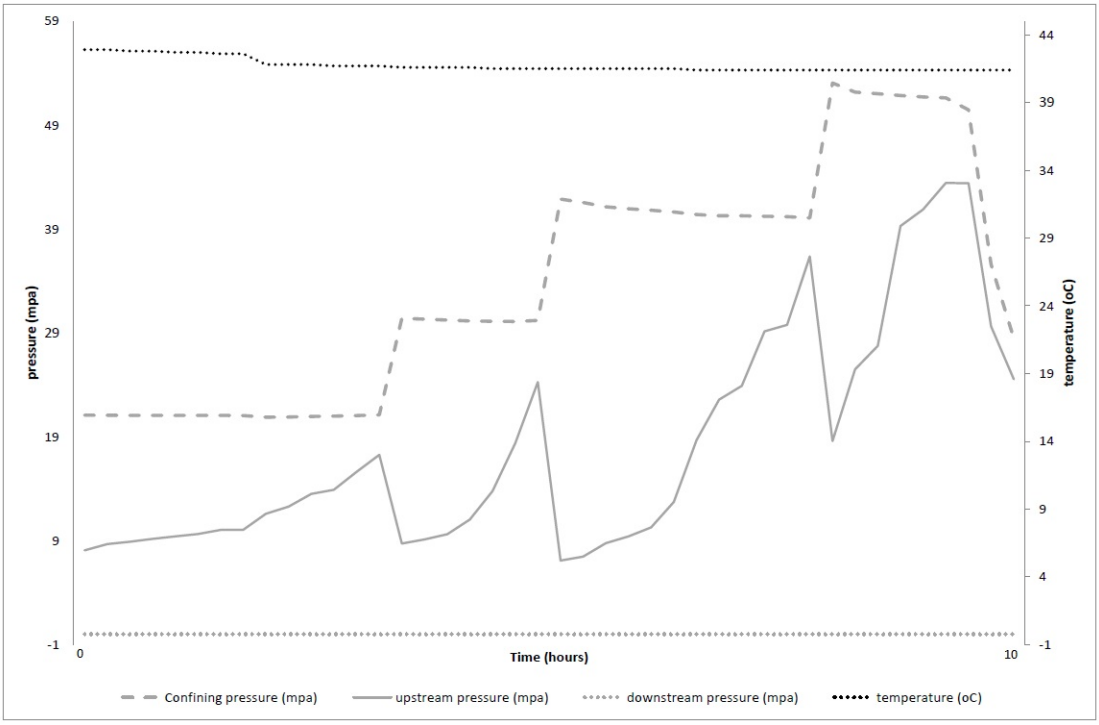

Figure 7a: Pressure plot for Phase 1, supercritical CO_2 flow experiment on Sample B-a. Note the downstream pressure remaining at atmospheric pressure indicates no flow through the sample.

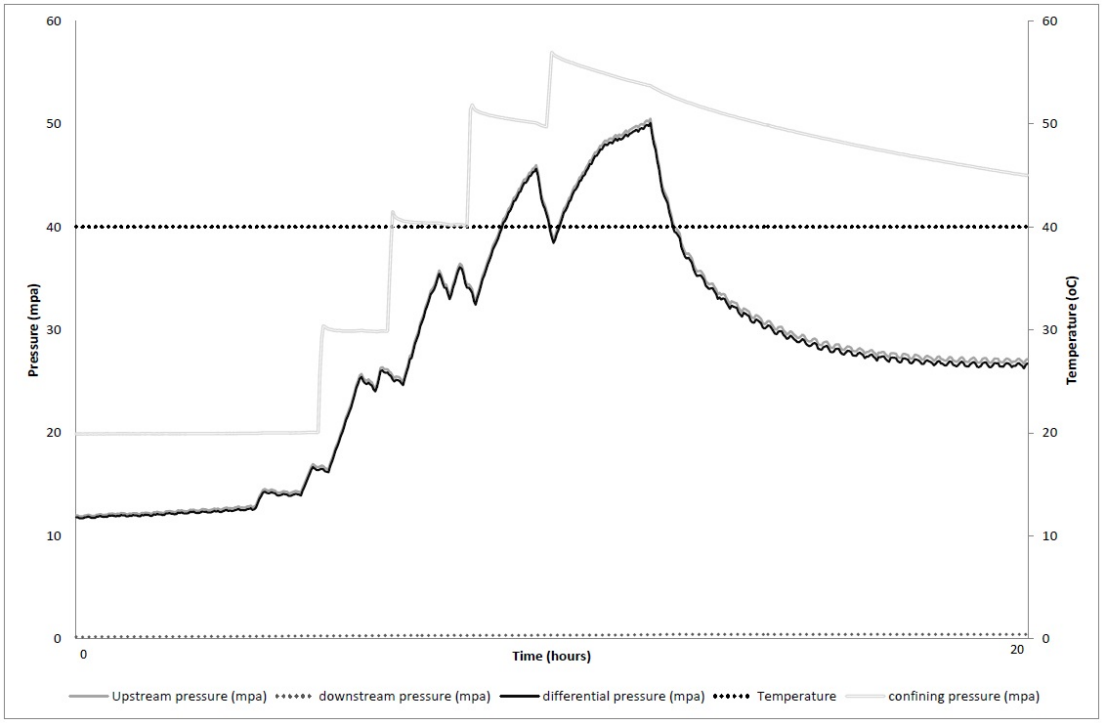

Figure 7b Pressure plot for Phase 1, supercritical CO_2 flow experiment on Sample B-b.

4.2. Phase 2: Supercritical CO_2 lock in results

The samples were locked into the pressure vessel and held constant above the supercritical point for 30 days at 10 MPa upstream fluid pressure, 40^{o}C and 25 MPa confining pressure, again the upstream and downstream pressures were measured and logged, Figure 8a and 8b.

There was negligible supercritical flow (pressure) measured across either of the fractured samples.

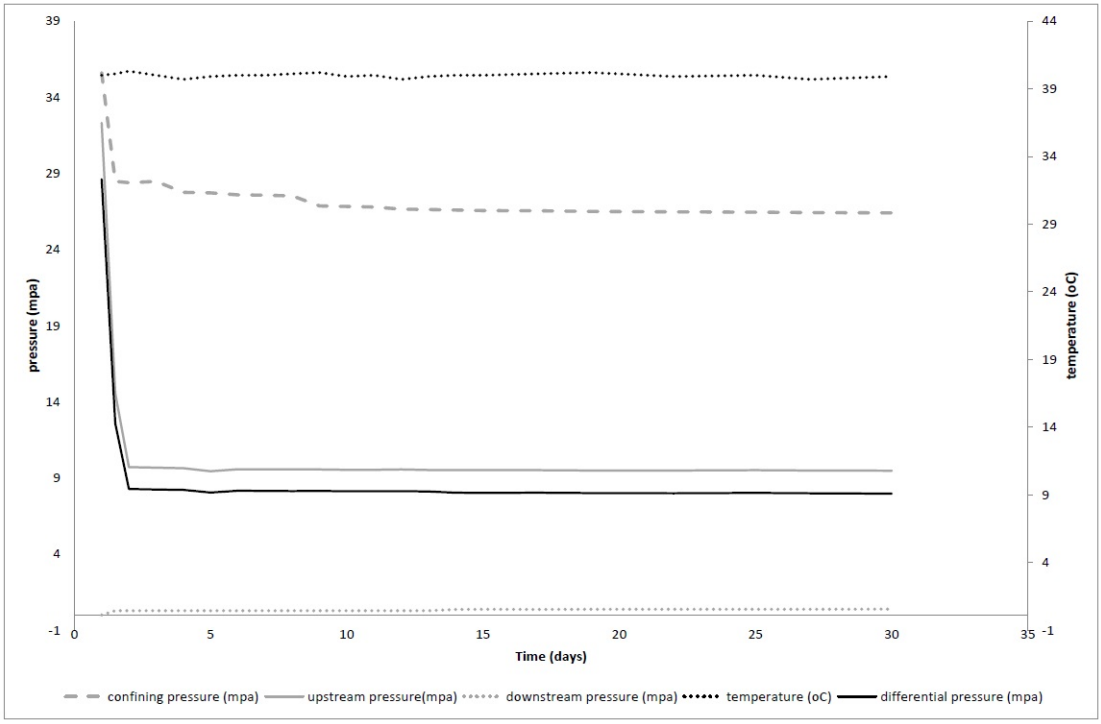

Figure 8a **:** Pressure plot for Phase 2, Constant supercritical CO_2 exposure for Sample B-a.

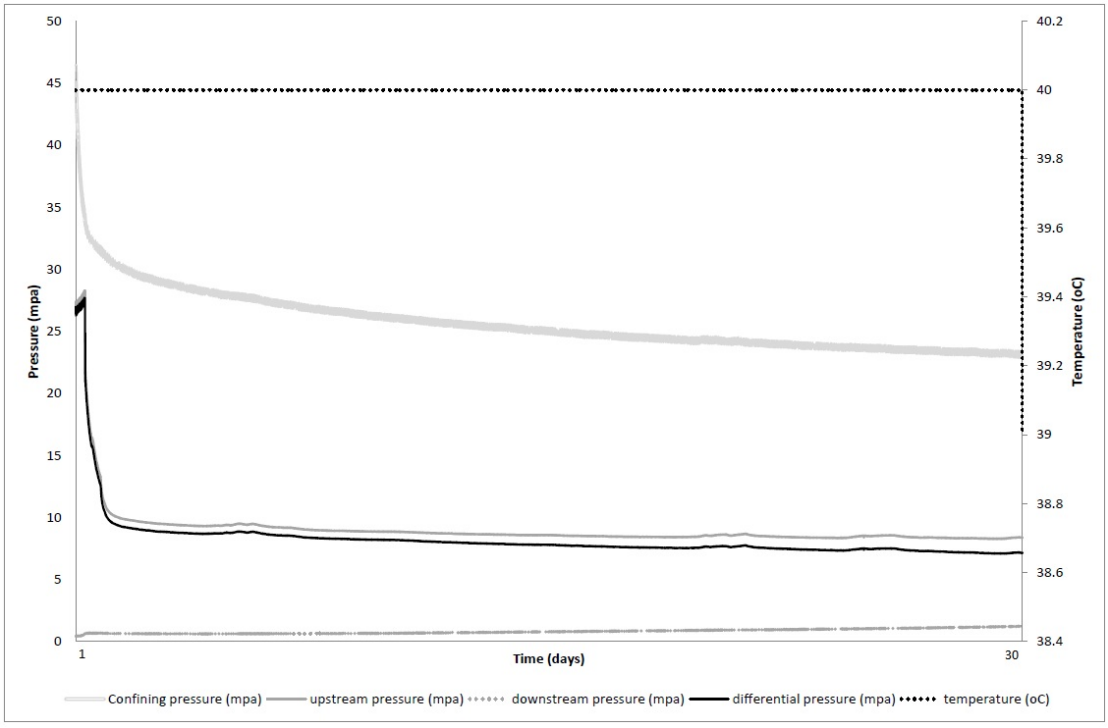

Figure 8b**:** Pressure plot for Phase 2, Constant supercritical CO_2 exposure for Sample B-b.

4.3. Phase 3: Gas phase CO_2 results

The upstream fluid pressure, confining pressure and fluid temperature were dropped below the critical point into the gas phase region and held constant at 6 MPa upstream fluid pressure, 20^{o}C and 15 MPa confining pressure for a further 30 days, again the upstream and downstream pressure were measured and logged, Figure 9a and 9b.

Once in the gas phase region the downstream pressure immediately and steadily increases over the 30 days to meet that of the upstream pressure and the associated differential pressure decreases.

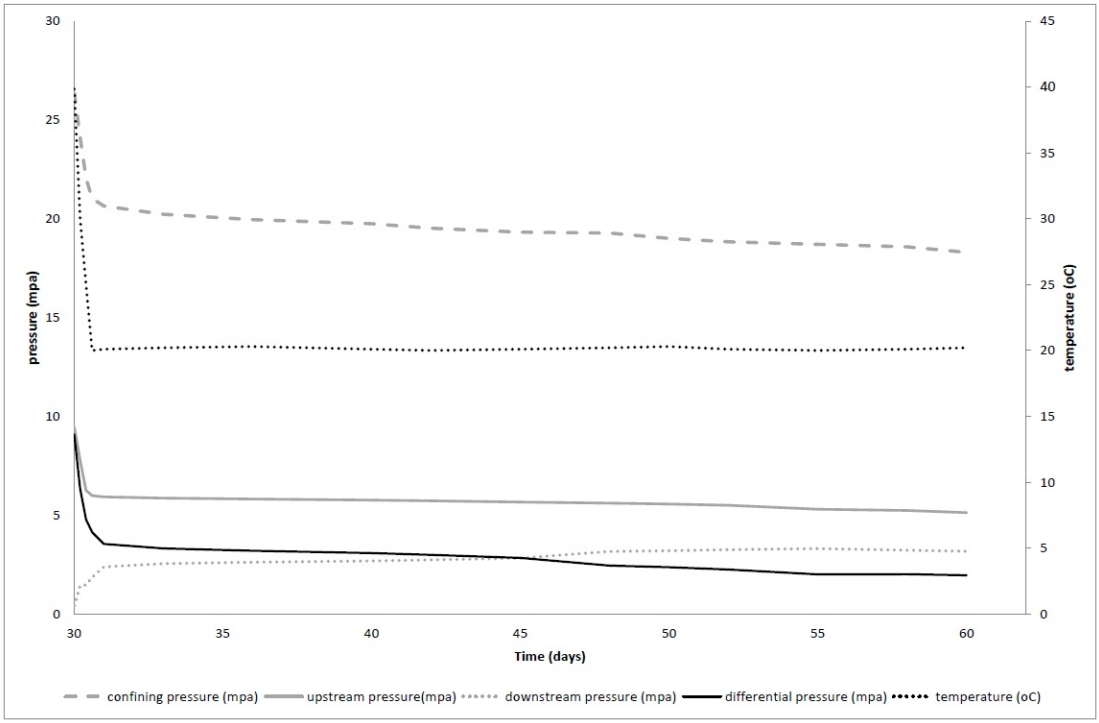

Figure 9a: Pressure plot for Phase 3, upstream fluid pressure, confining pressure and fluid temperature were dropped below the critical point into the gas phase region for Sample B-a.

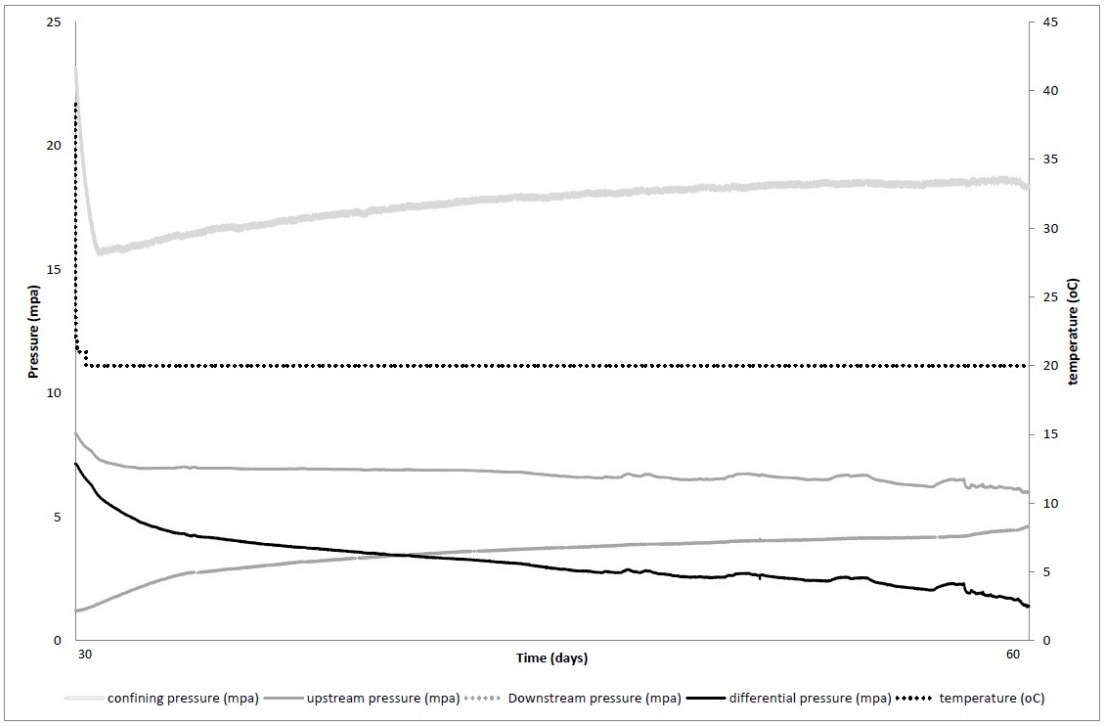

Figure 9b: Pressure plot for Phase 3, upstream fluid pressure, confining pressure and fluid temperature were dropped below the critical point into the gas phase region for Sample B-b.

4.4. Phase 4: Re-run of the increasing upstream CO_2 fluid pressure and lock in under supercritical conditions to investigate wettability changes

After 60 days exposure to gas phase CO_2 both of the fractured caprock samples were once again exposed to an increase in upstream CO_2 fluid pressure in 10 MPa increments from 20 MPa to 50 MPa and the samples were then locked in under supercritical conditions for 30 days and then finally the temperature and pressure was dropped into the gas phase region and locked in for a further 30 days. This was undertaken to see if there would be any $scCO_2$ flow along the fracture due to the CO_2 gas exposure along the fracture face influencing the wettability of the fracture face minerals which may then facilitate $scCO_2$ flow through the natural fractures.

There was minimal detectable flow of $scCO_2$ measured across both fractured samples under $scCO_2$ flow and lock in even with a pressure differential of 37 MPa and 41 MPa for samples B-a and B-b respectively, Figures 10a and 11a. Under gas phase lock in the similar pattern of increasing downstream pressure towards that of the upstream pressure was also observed, Figures 10b and 11b. Indicating that under the experimental conditions wettability (and in turn capillary entry pressures) of the fracture face were not influenced by exposure to gaseous CO_2.

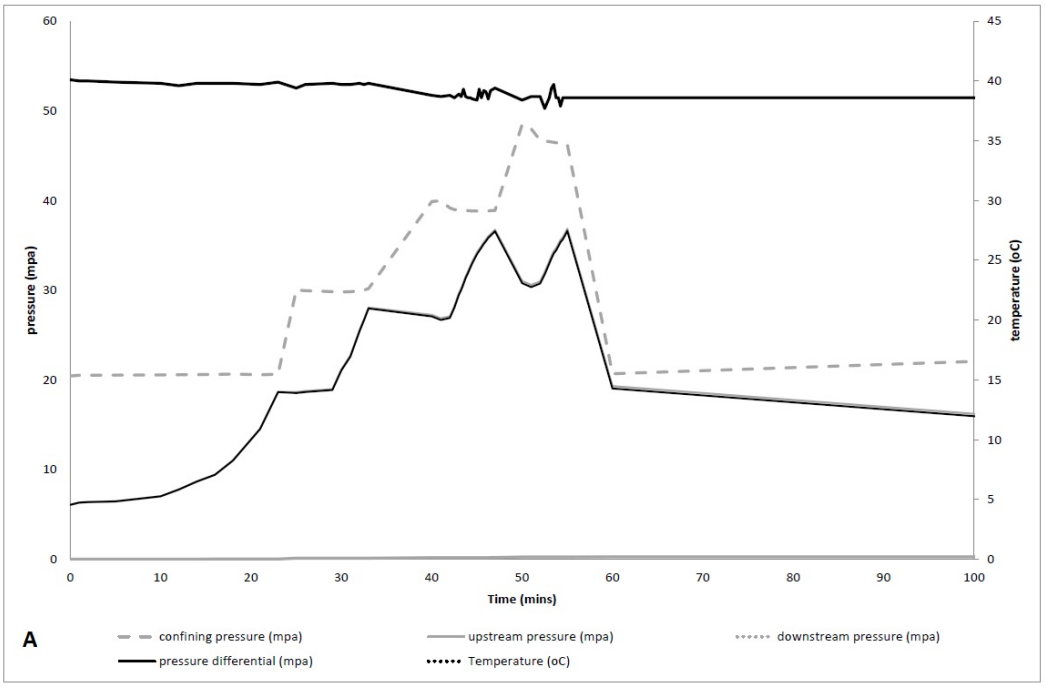

Figure 10a : Pressure plots for Phase 4, supercritical CO_2 flow in experiment for Sample B-a.

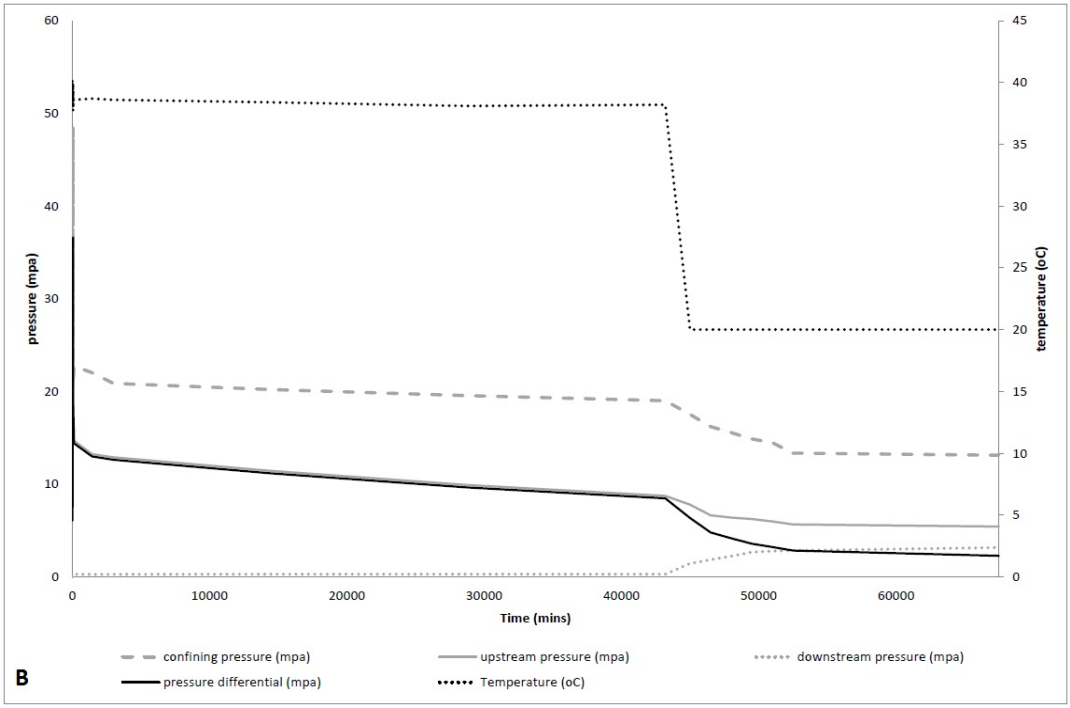

Figure 10b: Pressure plots for Phase 4, $scCO_2$ and gas CO_2 lock in experiment for Sample B-a.

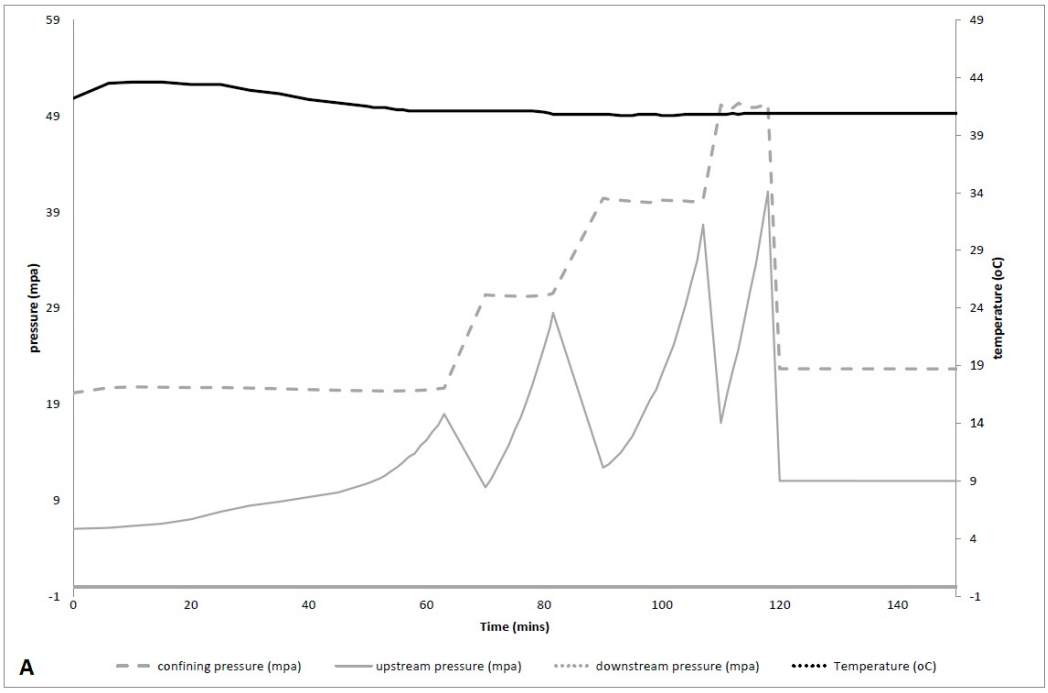

Figure 11a : Pressure plots for Phase 4, supercritical CO_2 flow experiment for Sample B-b.

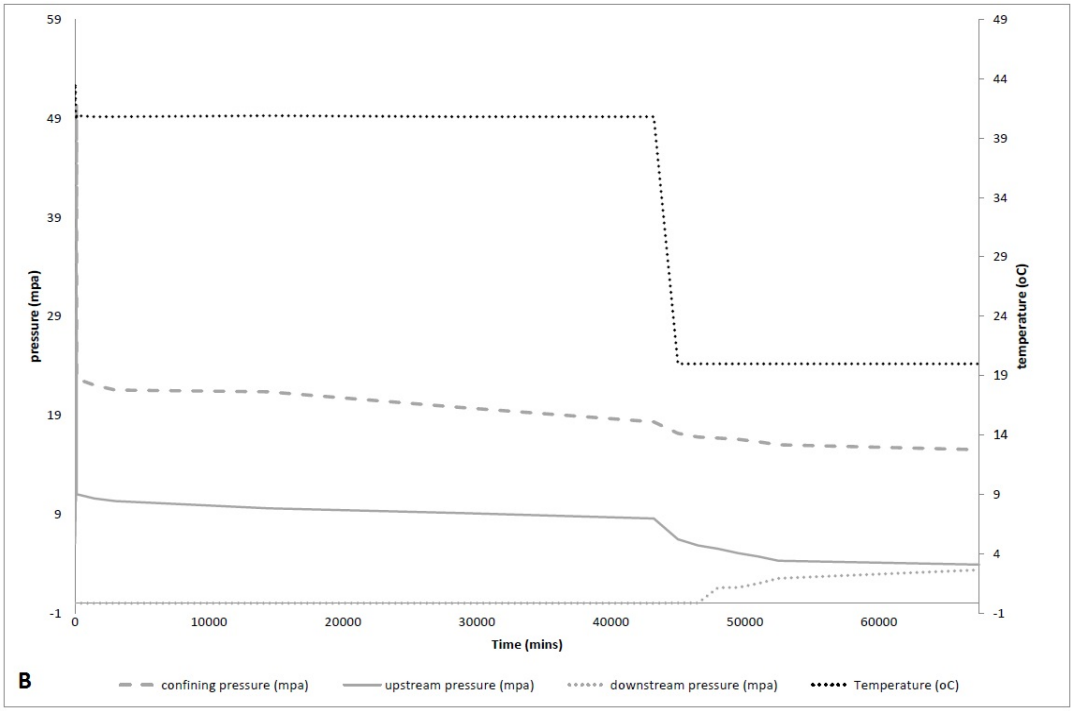

Figure 11b: Pressure plots for Phase 4, $scCO_2$ and gas CO_2 lock in experiment Sample B-b.

5. Discussion

At standard temperature and pressure, the density of carbon dioxide is 1.98 kg/m³, about 1.5 times that of air, (Span and Wagner,1996). At a temperature of 31.1°C and a pressure of

7.39 MPa CO_2 becomes supercritical. This is the equivalent of around 840 m depth assuming a geothermal gradient of 25°C/km and is exceeded under deep geological storage conditions.

The supercritical property of near liquid densities increases the probability of interactions between the carbon dioxide and the substrate, similar to a liquid solvent, (Fenghour et al. 1998). The gas-like diffusivities of supercritical CO_2 allow for increased mass transfer properties, indicating that supercritical CO_2 will penetrate a microporous matrix material, and that scCO_2 should flow through caprock fractures. However our initial experimental results contradict this behaviour for naturally fractured caprock under in-situ conditions.

Table 3 lists a summary of the pertinent factors involved in flow of CO_2 through fractured Kimmeridge Clay caprock under gas, liquid and supercritical pressure and temperature conditions. These values were used below to estimate flow through fractured caprock. In addition the values highlight areas of consensus and also areas where the data is incomplete or inconsistent.

Property	***p and T CO_2 Conditions***	***Values***	***Reference***
Dynamic Viscosity	Gas (5MPa / 35^{o}C)	16.89 10^{-6} Pa s	Fengour et al. (1998)
	Liquid (10MPa / 25^{o}C)	74.21 10^{-6} Pa s	Fengour et al. (1998)
	Supercritical (14MPa / 40^{o}C)	69.02 10^{-6} Pa s	Fengour et al. (1998)
Density	Gas (5MPa / 35^{o}C)	118.5 kg/m^3	Non ideal gas law
	Liquid (10MPa / 25^{o}C)	813 kg/m^3	Non ideal gas law
	Supercritical (15MPa / 35^{o}C)	396 kg/m^3	Non ideal gas law
IFT (water / CO_2)	Gas (4MPa / 35^{o}C)	44.2 ±0.0 mNm^{-1}	Bachu and Bennion (2009)
	Gas (5MPa / 35^{o}C)	44.3 ±0.7 mNm^{-1}	Chiquet et al. (2007)
	Gas (4.14MPa / 35^{o}C)	48.95mNm^{-1}	Chun and Wilkinson (1995)
	Gas (5MPa / 39.65^{o}C)	43.93 ±0.23 mNm^{-1}	Georgiadis et al. (2010)
	Gas (5MPa / 35^{o}C)	44.2 ±0.0	Hebach et al (2002)
	Gas (5MPa / 35^{o}C)		

		mNm^{-1} $39.3mNm^{-1}$	Kvamme et al (2007)
	Liquid (12MPa / 25°C) Liquid (10MP / 27°C) Liquid (10.34MPa / 25°C) Liquid (10MPa / 23°C) Liquid (10MP / 25°C)	26.5 mNm^{-1} 29.4 mNm^{-1} 27.41 mNm^{-1} 29.66 ± 0.2 mNm^{-1} 28.4 ±0.1 mNm^{-1}	Bachu and Bennion (2009) Chalbaud at al. (2009) Chun and Wilkinson (1995) Georgiadis et al. (2010) Hebach et al. (2002)
	Supercritical (12MPa / 35°C) Supercritical (15MPa / 35°C) Supercritical (15.5MPa / 35°C) Supercritical (15MPa / 39.65°C) Supercritical (15MPa / 35°C) Supercritical (12.MPa / 48.85°C)	18.6 mNm^{-1} 30.8 ±0.8 mNm^{-1} 25.79 mNm^{-1} 29.17 ±0.13 mNm^{-1} 28.5 ±0.0 mNm^{-1} 31.2 mNm^{-1}	Bachu and Bennion (2009) Chiquet et al. (2007) Chun and Wilkinson (1995) Georgiadis et al. (2010) Hebach et al. (2002) Kvamme et al (2007)
CO_2 contact angle for Quartz	Gas (5MPa) Gas (10MPa)	20^o 20^o	Espinoza and Santamarina (2010) Espinoza and Santamarina (2010)
CO_2 contact angle Calcite	Gas (5MPa) Gas (10MPa)	40^o 40^o	Espinoza and Santamarina (2010) Espinoza and Santamarina (2010)
Kimmeridge Clay Caprock pore throat		0.1 – 0.005microns	Okiongbo (2011)

radius			
Kimmeridge Clay Caprock Matrix permability	25 – nDarcy	0.1	Okiongbo (2011)

Table 3: Input parameters for Kimmeridge Clay rock properties and CO2 fluid properties

5.1. Fluid conductivity response of the fracture to the CO_2 phase

The fluid conductivity (similar to hydraulic conductivity except we include the fluid properties of the specific fluid rather than water) of the natural fracture to CO_2 in its gas, liquid and supercritical phase can be investigated using a simplified equation based on the cubic law, Witherspoon et al, (1979). Assuming flow is laminar along a parallel planar fracture the fluid conductivity of the fracture with an aperture 2b is given by:

$$K_f = (2b)^2 \rho g / 12\mu \qquad \text{Eqn. 1}$$

Where K_f is the fracture fluid conductivity (m/s), b the aperture half width (m), ρ the fluid density in (kg/m^3), g the acceleration of gravity (m/s^2) and μ the fluid viscosity (Pa s). Table 4 provides the input parameters for the gas, liquid and supercritical phase CO_2 and the calculated results of the fracture fluid conductivity for two different fracture apertures (half width of 10μm and 1μm) for each of the CO_2 phases.

Property	*CO_2 gas phase*	*CO_2 liquid phase*	*CO_2 supercritical phase*
Fluid viscosity (μ)	16.89 10^{-6} Pa s	74.21 10^{-6} Pa s	69.02 10^{-6} Pa s
Fluid density (ρ)	145 kg/m^3	810 kg/m^3	825 kg/m^3
Acceleration of gravity (g)	9.80665 m/s^2	9.80665 m/s^2	9.80665 m/s^2
Calculated fracture fluid conductivity (K_f)	**2.81 x10^{-3} m/s**	**3.56 x10^{-3} m/s**	**3.90 x10^{-3} m/s**

With *aperture half width of 10 µm*			
Calculated fracture fluid conductivity (K_f)	**2.81 x10^{-5} m/s**	**3.56 x10^{-5} m/s**	**3.90 x10^{-5} m/s**
With *aperture half width of 1 µm*			

Table 4: Input parameters and results for the hydraulic conductivity calculations under the different phases of CO_2 for two different fracture apertures.

It can be seen from the results in Table 4 that independent of aperture there is a variation in the conductivity between the three phases of CO_2. The calculated conductivity increases from the gas phase, through the liquid phase to the supercritical phase. However experimentally we do not observe an increase as the CO_2 moves from the gas phase into the supercritical phase.

5.2. Capillary entry pressure influenced by CO_2 phase

The Laplace law calculates the capillary entry pressure (P_c^{CO2}) value that has to be exceeded before the non-wetting phase can start to flow and is given by:

$$P_c^{CO2} = P_{CO2} - P_{brine} \approx 2\gamma\cos\theta / r_{throat}^{\max} \qquad \text{Eqn. 2}$$

Where γ is the brine/CO_2 IFT between the two fluids, θ is the contact angle (measured in the brine, wetting, phase) of the mineral / brine / CO_2 system and $r_{throat}^{\max}$ is the largest connected pore throat radius (or microfracture) in the caprock.

In general storage caprocks and natural fractures have very small pore throat sizes (0.1 to 0.005 µm, Nelson (2009)) and very low permeabilities (25 – 0.1 nDarcy, (Schlomer and Kroos, 1997)), therefore the sealing efficiency of the fractured caprock primarily depends on the IFT and the contact angle.

The IFT of the two phase system (CO_2 / water) has been studied intensively. While the water phase can be regarded as nearly incompressible the CO_2 phase is highly compressible. Therefore pressure and temperature have an effect on the IFT in this system. IFT experimental values have been reported by Hocott (1938), Heuger (1957), Chun et al (1995), Ren et al. 2000, Yan et al. (2001), Kvamme et al. (2007), Hildenbrand et al. (2004), Bennion and Bachu (2006), Chiquet et al (2006, 2007), Chalbaud (2006, 2009) and Georgiadis et al, (2010). They show that under pressure and temperatures equivalent to storage depths of up

to 2000 m the CO_2 / water IFT's have values above 20 mN/m and are approximately independent of pressure and decreases very slowly with temperature. Increasing salinity slightly increases the IFT, therefore it can be inferred that capillary sealing efficiency are improved by storing CO_2 at higher depths (Chiquet et al, 2006).

The contact angle arises as a surface chemistry effect and is therefore a function of the rock as well as the two fluid phases. A strongly water wet system has a contact angle of 0^o. The Young-Dupree equation relates the contact angle (θ) to the IFT's of the fluid-liquid (γ_{fl}), fluid-solid (γ_{fs}), and liquid-solid (γ_{ls}), systems:

$$\cos\theta = (\gamma_{fs} - \gamma_{ls}) / \gamma_{fl} \qquad \text{Eqn. 3}$$

Changes in IFT with CO_2 pressure alter the contact angle in the mineral / brine / CO_2 system. Work by Chun and Wilkinson (1995), Cai et al. (1996), Chiquet et al (2006 and 2007), Chalbaud et al (2009, 2009) and Espinoza and Santamarina (2010) have shown that in the presence of CO_2 contact angles reveal a transition from water-wet behaviour at low pressures (gas CO_2) towards an intermediate wettability at high pressure (>10MPa, supercritical CO_2) that is more pronounced for mica than quartz. Over the pressure interval 0-11MPa the contact angle variation is in the order of 40-50^o for mica and 15 – 25^o for quartz, at high pressure mica is less water wet than quartz. Espinoza and Santamarina (2010) have also noted that the contact angles between $CO_{2liquid}$ / water and $CO_{2liquid}$ / solid approach $\theta \approx 0$ in a vapour-CO_2 atmosphere. In terms of reservoir integrity, the changing wetting behaviour under pressure of the CO_2 could lead to an earlier capillary breakthrough through the caprock (from Eqn. 2).

Taking Equation 2 and calculating the capillary entry pressure for the three different phases of CO_2 using the data in Table 3, and assuming a water-wet calcite with contact angle of 40^o and a largest connected fractured caprock fill throat radius of 1micron, we see a trend of decreasing capillary entry pressure towards the supercritical phase, Table 5.

Property	*CO_2 gas phase*	*CO_2 liquid phase*	*CO_2 supercritical phase*
Interfacial tension	44 mNm^{-1}	29 mNm^{-1}	30 mNm^{-1}
Water wet calcite – contact angle	40	40	40
Largest connected throat radius	0.000001 m	0.000001 m	0.000001 m

Capillary entry pressure **With largest connected throat radius 1µm**	**88MPa**	**58MPa**	**60MPa**

Table 5: Input parameters and results for the capillary entry pressure calculations for the different phases of CO_2 under idealised condition.

The fact that the gas phase CO_2 has a larger capillary entry pressure than the supercritical phase CO_2 further suggests that in our experiments the $scCO_2$ should have flowed more easily through the samples than the gas.

6. Analogue Field Studies

A number of field scale observations of CO_2 leakage sites (publication in press) indicate that there is no CO_2 leakage from deep CO_2 storage reservoirs, however there is CO_2 gas leakage from the shallower reservoirs. Lewicki et al. 2007 make the general observation that leakage seems to be restricted to relatively shallow (in their case < 2000m) reservoirs.

The implications of these results suggest that if supercritical CO_2 does migrate from the storage site and travels towards the surface, leakage will be restrained until the in-situ conditions of pressure and temperature fall below the critical point of 7.35MPa and 31^{o}C (the equivalent of around 840m depth assuming a geothermal gradient of 25°C/km) when there is likely to be leakage through caprock fractures of CO_2 in its gaseous phase

7. Conclusions

The conclusions we can draw from the experimental work undertaken so far on multiphase flow of CO_2 in fractured caprocks are that:

- Initial results indicate that supercritical CO_2 does not flow through tight natural caprock fractures under in-situ reservoir conditions.
- When the temperature and fluid pressure are reduced to below the critical point, CO_2 in its gas phase does flow through the tight caprock fractures.
- There is the possibility that there is a threshold of fracture aperture which allows gas CO_2 flow but not supercritical CO_2 flow under in-situ conditions of pressure and temperature.
- This has significant implications for the planning of CO_2 storage projects in the North Sea basin, in that the CO_2 must be stored at pressures and temperatures (depth) comfortably above the CO_2 critical point.

The definition of a supercritical fluid is that there is no phase boundary between the liquid and gas phases, that the fluid will pass through solids like a gas, but will have liquid densities. We have found experimentally however that supercritical CO_2 is not flowing through the naturally fractured caprock as a gas as we would have expected it to.

We note that the pressure gradients applied on the samples are extremely high and unlikely to occur in nature. This makes the findings even more relevant in that we have tried to force supercritical CO_2 flow under extreme conditions and have not been successful.

7.1. Future work

The work has raised a number of questions which will be addressed by further work including:

- More experiments of additional naturally fractured caprock samples from different wells and different caprock types over longer timescales to ensure these are not isolated observations.
- Experiments run on artificially fractured caprock samples, with varying fracture apertures to determine whether there is a threshold of fracture spacing which allows gas flow but not supercritical CO_2.
- Undertake further geochemical investigations into the influence of gas and supercritical phase CO_2 on the wettability of real caprock samples under in-situ storage conditions of temperature and pressure.
- Tie in experimental measurements with field analogue observations.
- Investigate the possibility of "spiking" CO_2 with molecules such as noble gasses which will remain gaseous under normal reservoir conditions and thereby act as markers able to migrate through fracture systems in the caprock otherwise closed to supercritical CO_2 flow. The use of such molecules could operate as a monitoring technique for determining the location of a CO_2 plume.

8. Acknowledgements

The research leading to these results has received funding from the European Community's Seventh framework Programme FP7/2007-2013 under the grant agreement No. 227286 MUSTANG - A Multiple Space and Time scale Approach for the quantification of deep saline formations for CO2 storage and from the Scottish Funding Council for the Joint Research Institute with the Heriot-Watt University which is part of the Edinburgh Research Partnership in Engineering and Mathematics (ERPem). We would like to acknowledge the generous support of Marathon Oil UK Ltd for providing the Kimmeridge Clay caprock samples.

9. References

Al-Bazali, T.M., Zhang, J., Chenevert, M.E. and Sharma, M.M., 2005. Measurement of the Sealing Capacity of Shale Cap-rocks, SPE 96100, presented at the SPE Annual Technical Conference and Exhibition held in Dallas, Texas, U.S.A., October 09–12.

Amann, A., Waschbüsch, M., Bertier, P., Busch, A., Kroossa, B.M., Littke R., 2011. Sealing rock characteristics under the influence of CO_2, Energy Procedia. 4, 5170–5177.

Angeli, M., Soldal, M., Skurtveit, E. and Aker, E., 2009. Experimental percolation of supercritical CO_2 through a caprock. Energy Procedia. 1, 3351–3358.

Bachu, S. 2003: Screening and ranking sedimentary basins for sequestration of CO_2 in geological media in response to climate change. Environmental Geology, 44**,** pp 277−289.

Bachu S. and Bennion B., 2009. Interfacial tension between CO2, freshwater and brine in the range of pressures from (2 to 27)MPa, temperature from (20 to 125)C and water salinity from (0to 334000)mg.L^{-1}J. Chem. Eng. Data 54. P.765-775.

Bennion, B. and Bachu, S., 2006. Supercritical CO_2 and H_2S-brine drainage and imbibition relative permeability relationships for intergranular sandstone and carbonate formations. in SPE Europec/EAGE Annual Conference and Exhibition, Vienna, Austria, 12-15 June 2006.

Bennion, B. and Bachu, S., 2007. Permeability and relative permeability measurements at reservoir conditions for CO_2-water systems in ultralow-permeability confining caprocks. in SPE Euopec-EAGE Annual Conference, 11-14 June 2007. London, UK.

Branter, S. R. F., 2003. The East Brae Field, Blocks 16/03a, 16/03b, UK North Sea in Gluyas, J. G. & Hichens, H. M. (eds). United Kingdom Oil and Gas Fields Commemorative Millennium Volume. Geological Society. London. Memoir 20, pp. 191-197.

Blanpied, ML, Lockner, DA, Byerlee, JD. 1992. An earthquake mechanism based on rapid sealing of faults. Nature 358, pp. 574–6.

Bouvier, J.D, Sijpesteijn, K, Kleusner, D.F, Onyejekwe, C.C, van der Pal, R.C. 1989.Three-dimensional seismic interpretation and fault sealing investigations, Nun River field, Nigeria. American Association of Petroleum Geologists Bulletin, 73, pp. 1397–1414

Busch, A., Amann, A., Bertier, P., Waschbusch, M. and Kroos, B.M., 2010. The Significance of Caprock Sealing Integrity for CO_2 Storage. SPE 139588

Cai, BY, Yang, JT, Guo, TM., 1996. Interfacial temperature of hydrocarbon + water/brine systems under high pressure. J Chem Eng Data 41. pp. 493-496.

Chadwick, A., Arts, R., Bernstone, C., May, F., Thibeau, S. & Zweigel, P. 2008. Best Practise for the Storage of CO2 in Saline Aquifers - Observations and guidelines from the SACS and CO2STORE projects. *North Star*. BGS.

Chalbaud, C., Robin, M. and Egermann, P., 2006. Interfacial tension of CO2/brine systems at reservoir conditions in: Gale, J. Rokke, N. Zweigel P. and Swenson H. (eds) Proceedings of the 8th International Conference on Greenhouse Gas Control techn. Elseiver, Amsterdam.

Chalbaud, C., Robin, M., Lombard, J.M., Martin, F., Egermann, P. and Bertin, H., 2009. Interfacial tension measurements and wettability evaluation for geological CO2 storage. Advances in Water Resources, 32, 98-109.

Chiquet, P., Broseta, D. and Thibeau, S. 2007. Wettability alteration of caprock minerals by carbon dioxide. Geofluids. 7, 112-122.

Chiquet, P., et al., 2006. CO_2/water interfacial tensions under pressure and temperature conditions of CO_2 geological storage. Energy Conversion and Management. p. 736-744.

Chun, B.B. and Wilkinson, G.T. 1995. Interfacial tension in high pressure carbon dioxide mixtures. Ind. Eng. Chem.. res. 34, 4371-4377.

Class, H. (Ed.) 2009. A benchmark study on problems related to CO_2 storage in geologic formations, Summary and discussion of the results Comput Geosci. 13, 409–434.

Deming, D., 1994. Factors necessary to define a pressure seal. AAPG Bulletin. 78(6): pp. 1005-1009.

Espinoza, D. N. and Santamarina, J.C., 2010. Water - CO_2 - mineral systems: Interfacial tension, contact angle, and diffusion – implications to CO_2 geological storage. Water Resources Research. Vol 46.

Fenghour A., Wakeham, W.A. and Vesovic V., 1998. The viscosity of Carbon Dioxide. J. Phys. Chem. Ref. Data, Vol. 27 No.1 pp. 31-44.

Fischer, S., Liebscher, A. and Wandrey, M., 2010. CO_2–brine–rock interaction: First results of long-term exposure experiments at insitu P–T conditions of the Ketzin CO_2 reservoir. Chemie der Erde 70, S3, 155–164.

Gaus, I. 2010. Role and impact of CO_2–rock interactions during CO_2 storage in sedimentary rocks, International Journal of Greenhouse Gas Control, 4, 73–89.

Georgiadis, A., Maitland, G., Trusler J.P. and Bismark A. 2010. Interfacial tension measurements of the (H_2O + CO_2) system at elevated temperatures and pressures. J. Chem. Eng Data, 55. Pp4168 – 4175.

Gunter, W. D., Bachu, S. & Benson, S. 2004. The role of hydrogeological and geochemical trapping in sedimentary basins for secure geological storage of carbon dioxide. *Geological Society, London, Special Publications,* 233**,** 129-145.

Handin, J., Hager, Jr R.V., Friedman, M., Feather, JN., 1963. Experimental deformation of sedimentary rocks under confining pressure: pore pressure tests. Bull Am Assoc. Petrol. Geol. 47(5):717–55.

Hebach, A., Oberhof, A., Dahmen, N., Kogel, A., Ederer, H. and Dinjus, E. 2002. Interfacial tension at elevated pressures; measurements and correlations in the water and carbon dioxide system. J. Chem. Eng. Data 47, 1540-1546.

Heuger, G.J., 1957. Interfacial tension of water against hydrocarbon and other gases and adsorption of methane and solids at reservoir conditions, PhD disertation, The University of Taxas, Austin.

Hildenbrand, A., Schloemer, S., Krooss, B.M. and Littke, R., 2004. Gas breakthrough experiments on pelitic rocks: comparative study with N_2, CO_2 and CH_4. Geofluids. 4, 61–80.

Hocott, CR., 1938. Interfacial tension between water and oil under reservoir conditions up to pressures of 3800psi and temperature of 180^{o}F AIME Trans 132, p 184-190.

IEA, Energy Technology Perspective (2008a).

Katsube, T.J. and Connell, S. 1998. Shale permeability characteristics; in Current Research 1998-E Geological Survey of Canada p. 183-192.

Ketzer, J.M., Iglesias, R., Einloft, S., Dullius, J., Ligabue, R. and De Lima, V. 2009. Water–rock–CO_2 interactions in saline aquifers aimed for carbon dioxide storage: Experimental and numerical modelling studies of the Rio Bonito Formation (Permian), southern Brazil. Applied Geochemistry. 24, 760–767.

Koide, H., Tazaki Y., Noguchi Y., Nakayama S., Iijima M., Ito K. and Shindo Y. 1992. Subterranean containment and long term storage of carbon dioxide in unused aquifers and in depleted natural gas reservoirs. Energy Convers. Manag. 33 (5-8), 619-626.

Kvamme, B., et al., 2007. Measurements and modelling of interfacial tension for water + carbon dioxide systems at elevated pressures. Computational Materials Science. **38**(3): p. 506-513.

Lewicki, J., Birkholzer, J. and Tsang, C-F., 2007, Natural and industrial analogues for leakage of CO2 from storage reservoirs: identification of features, events, and processes and lessons learned, Environmental Geology, v 52, no. 2, p 457-467.

Li, S., Dong, M., Li, Z., Huang, S., Qing, H., Nickel, E., 2005. Gas breakthrough pressure for hydrocarbon reservoir seal rocks: implications for the security of long-term CO_2 storage in the Weyburn field. Geofluids. 5: p. 326-334.

Li, Z., Dong, M., Li, S., Huang, S., 2006. CO_2 sequestration in depleted oil and gas reservoirs—caprock characterization and storage capacity. Energy Conversion and Management. 47: p. 1372–1382.

Lindsay, N.G, Murphy, F.C, Walsh, J.J, Watterson, J. 1993. Outcrop studies of shale smears on fault surfaces. International Association of Sedimentologists, Special Publication, 15, pp. 113–123

McDermott, C. I., Randriamanjatosoa, A. R.L., Tenzer, H. and Kolditz, O. 2006. Simulation of heat extraction from crystalline rocks: The influence of coupled processes on differential reservoir cooling. Geothermics 35 321–344.

Nelson, P.H., 2009. Pore-throat sizes in sandstones, tight sandstones and shales. AAPG Bulletin, v. 93, no. 3 (March 2009), pp. 329–340 329.

Muller, N. 2011 Supercritical CO_2-brine relative permeability experiments in reservoir rocks – literature review and recommendations. Transport in Porous Media. 87 367-383.

Nygard, R., Gutierrez, M., Bratli, R.K. and Høeg, K. 2006. Brittle–ductile transition, shear failure and leakage in shales and mudrocks. Marine and Petroleum Geology. 23, 201–212.

Okiongbo, K.S., 2011. Bulk volume reduction of the Kimmeridge Clay Formation, North Sea (UK) due to compaction, petroleum generation and expulsion, Research Journal of Applied Sciences, Engineering and Technology 3(2): 132-139.

Pruess, K. 2008 Leakage of CO_2 from geologic storage: Role of secondary accumulation at shallow depth. Int. J. Greenhouse Gas Control 2 (1) 37-46.

Ren, QY., Chen, GJ., Yan, W., Guo, TM., 2000. Interfacial tension of (CO_2+CH_4)+water from 298K to 373K and pressures up to 30MPa. J. Chem Eng Data 45, p. 610-612.

Schowalter, T. T. 1981. Prediction of cap rock seal capacity. Bulletin, American Association of Petroleum Geologists 65:987.

Schlomer S. and Kroos B.M. 1997 Experimental characterisation of the hydrocarbon sealing efficiency of cap rocks. Marine and Petroleum Geology. Vol 14 No.5 p.565-580.

Span, R., and Wagner, W., 1996. A new equation of state for carbon dioxide covering the fluid region from the triple-point temperature to 1100 K at pressures up to 800 MPa. Journal of Physical and Chemical Reference Data 25(6): 1509-1596.

UK Met Office Data, 2010 - www.metoffice.gov.uk/climatechange

Watts, N.L., 1987, Theoretical aspects of cap rock and fault seals for single and two phase hydrocarbon columns: Marine and Petroleum Geology, v. 4, p. 247-307.

Wollenweber, J., Alles, A., Busch, A., Krooss, B.M., Stanjek, H. and Littke, R. 2010. Experimental investigation of the CO2 sealing efficiency of caprocks. Int. Journal of Greenhouse gas Control. 4, 231-241.

Wollenweber, J., Alles, S., Kronimus, A., Busch, A., Stanjek, H. and Krooss, B.M. 2009. Caprock and overburden processes in geological CO_2 storage: an experimental Study Energy Procedia. 1, 3469 – 3476.

Witherspoon, P.A, Wang J.S.Y., Kwai, K. Gale, J.E. 1979 Validity of cubic law for fluid flow in a deformable rock fracture. Water Resource Research.

Yan, W., Zhao, G-Y., Chen, G-J., Guo, T-M. 2001. Interfacial tension of (methane+nitrogen)+water and (carbon dioxide+nitrogen)+water systems. J Chem Eng Data 46, p1544-1548.

Yang, Y. and Aplin, A.C. 2007. Permeability and petrophysical properties of 30 natural mudstones Journal of Geophysical Research. Vol. 112.

Yielding, G., Freeman, B. and Needham, D.T. 1997. Quantitative fault seal prediction. American Association of Petroleum Geologists Bulletin, 81, pp. 897–917.